AGU ADVANCING EARTH AND SPACE SCIENCES

Geophysical Research Letters

RESEARCH LETTER
10.1029/2023GL104663

The Repetition Period of MeV Electron Microbursts as Measured by SAMPEX/HILT

Hamdan Kandar[1], Lauren Blum[1,2], Mykhaylo Shumko[3], Lunjin Chen[4], and Jih-Hong Shue[5]

[1]University of Colorado Boulder, Boulder, CO, USA, [2]Laboratory for Atmospheric and Space Physics, Boulder, CO, USA, [3]The Johns Hopkins University Applied Physics Laboratory, Laurel, MD, USA, [4]University of Texas Dallas, Richardson, TX, USA, [5]Department of Space Science and Engineering, National Central University, Jhongli, Taiwan

Key Points:

- The repetition period of MeV electron microbursts is studied for the first time using 15 years of Solar, Anomalous, Magnetospheric Particles Explorer/Heavy Ion Large Telescope data
- Microburst repetition periods are most often <1 s, and drop off as a power law moving to longer periods
- Repetition periods show strong agreement with chorus wave element periodicities in all magnetic local time sectors except for the dusk sector

Correspondence to:

H. Kandar,
Haka8022@colorado.edu

Citation:

Kandar, H., Blum, L., Shumko, M., Chen, L., & Shue, J.-H. (2023). The repetition period of MeV electron microbursts as measured by SAMPEX/HILT. *Geophysical Research Letters*, *50*, e2023GL104663. https://doi.org/10.1029/2023GL104663

Received 6 JUN 2023
Accepted 28 SEP 2023

Abstract

Here we examine properties of MeV electron microbursts to better understand their generation mechanisms. Using 15 years of data from Solar, Anomalous, Magnetospheric Particles Explorer/Heavy Ion Large Telescope, >1 MeV microburst repetition periods (time spacing between bursts) are examined and clear dependencies on Auroral Electrojet (AE), L shell, and magnetic local time (MLT) are discovered. Microburst repetition periods are shortest around 0–6 hr MLT and 4–5 L shell, and grow longer toward the day and afternoon sectors and larger L shells. Shorter repetition periods (<1 s) are also found to be more common during higher AE, while longer periods (>10 s) more common during quiet times. The microburst repetition period distributions are compared directly to those of rising tone chorus wave elements and found to be similar in the night, dawn and day MLT sectors, suggesting chorus wave repetition periods are likely directly controlling those of microburst precipitation. However, dusk-side distributions differ, indicating that the dusk-side microbursts properties may be controlled by other processes.

Plain Language Summary

Looking at energetic electrons in Earth's magnetosphere from the Heavy Ion Large Telescope instrument on board the Solar, Anomalous, Magnetospheric Particles Explorer satellite helps us better understand the feature called microbursts. Microbursts are very rapid bursts of enhanced high-energy electrons entering our atmosphere. In this study, we characterize the properties of the microbursts to understand when, and where they happen, what causes them, and what impact they might have. We do so by looking at factors such as their magnetic local time as well as their time separation. This study also compares these microbursts' results to previous chorus wave studies. Chorus waves have been thought to be related to microbursts and could be a cause for some of their properties. We discuss more about this correlation in the result section of this study.

1. Introduction

Microbursts are rapid (sub-second) bursts of energetic electrons entering Earth's atmosphere from the magnetosphere. They have been shown to be a significant source of loss for the radiation belts during storm main and recovery phases (e.g., Blum et al., 2015; Breneman et al., 2017; O'Brien et al., 2004; Thorne et al., 2005), as well as a potential driver of mesospheric Ozone loss (Duderstadt et al., 2021; Seppälä et al., 2018). Microbursts have been observed by numerous spacecraft in low Earth orbits, and can range from keV up to MeV energies (Elliott et al., 2022 and references within). Microbursts occur most frequently between 4 and 6 L shell and from midnight to morning (0–12 hr) magnetic local time (MLT) (Lorentzen et al., 2001; Nakamura et al., 2000). They typically last on the order of 100 ms, and estimates of the physical size of individual microbursts are on the order of 10 km (e.g., Crew et al., 2016; Shumko et al., 2018, 2020, 2021).

Due to their similar distributions in L shell and MLT, as well as their short sub-second durations, rising tone chorus waves have long been considered a primary mechanism for generating microbursts. Chorus waves have been shown to be able to resonate with energetic electrons, rapidly scattering them into the loss cone. Gyro-resonant with keV electrons close to the magnetic equator, and as chorus wave packets propagate to higher magnetic latitudes they can resonate with higher energy (MeV) electrons (e.g., Horne & Thorne, 2003; Saito et al., 2012). Simulations as well as a handful of observations have shown a close correspondence between chorus waves in the magnetosphere and relativistic electron microbursts at low altitudes (e.g., Breneman et al., 2017; Chen et al., 2022; Miyoshi et al., 2020; Mozer et al., 2018).

Microbursts typically occur in rapid succession, often referred to as microburst trains (e.g., O'Brien et al., 2004). It is still an open question what determines the time spacing (or repetition period) of trains of microbursts, as well as whether isolated microbursts are generated by the same mechanisms as trains. In this work, we explore the repetition period of MeV electron microbursts, to gain insight into the possible generation mechanisms for these repetition periods. Using 15 years of data from the Solar, Anomalous, Magnetospheric Particles Explorer (SAMPEX) satellite, we calculate the repetition period of MeV microbursts and examine its dependence on L shell, MLT, and Auroral Electrojet (AE). We then compare these patterns to those found in previous studies of chorus wave properties.

2. Methodology

2.1. Detecting Microbursts

The SAMPEX satellite was designed to measure energetic nuclei and electrons over a broad dynamic range (Baker et al., 1993). SAMPEX was launched 3 July 1992 into an 82 degree inclination low altitude orbit carrying four instruments From this high inclination, the SAMPEX orbit provides coverage beyond 10 L shell and predesses in local time every ∼6 months, providing comprehensive coverage of the outer radiation belt from low Earth orbit. We use 20 ms cadence measurements of >1 MeV electrons from the Heavy Ion Large Telescope (HILT) (Klecker et al., 1993; SAMPEX/HILT, 2013) to detect relativistic electron microbursts from 1997 to 2012.

To detect microbursts in the SAMPEX/HILT data, we apply an algorithm developed by O'Brien (2003) and applied in a number of previous studies:

$$(N_{100} - A_{500})/\sqrt{1 + A_{500}} > 10$$

where N_100 is the number of counts in 100 ms and A_{500} is a running average over 500 ms. The threshold of the above ratio set to be 10 so that most microbursts are picked up while false detections are minimized. For each microburst time, if in the surrounding 250 HILT samples (nominally 5 s), there exists a data gap with duration exceeding 1 s, we discard that microburst detection, in order to remove false detections near data gaps. Applying this algorithm to the 15 years analyzed results in a total of 279,061 microburst detections. This database of microbursts detected by SAMPEX/HILT, while it was in State 4 (20 ms cadence) and while SAMPEX was not spinning, was compiled by and is available in Shumko et al. (2021), Shumko (2020).

2.2. Calculating the Repetition Period

Once we have the list of microburst detections with assigned date and time, we then calculate the time between each microburst (denoted as dt). Figure 1a shows the application of the O'Brien (2003) microburst detection algorithm as applied to SAMPEX data, as well as how the repetition period (dt) is estimated. Figure 1b shows the overall distribution of dt's during the 15 year period analyzed. We see from this that most microbursts occur less than one second apart. The number of microbursts drops off as a power law when moving to larger time separations, with slope ∼−1.48.

3. Results

3.1. L Shell and MLT Dependence

With the large database of microbursts and their time separations (dt's) produced in the steps above, we now explore how the distribution of dt varies with location and geomagnetic activity.

Figure 2a shows the distribution of overall microburst in MLT and L shell. The number of microburst detections are binned into 1 L by 1 MLT bins. Microbursts are most frequent on the morning side of the magnetosphere, from ∼4 to 6 L shell, in good agreement with past studies (O'Brien, 2003). This figure also shows that even in the afternoon sector, more than ∼100 detections go into bins from 4 to 6 L shell, providing sufficient statistics for examining microburst repetition periods away from their location of peak occurrence as well.

Figure 2b shows the median dt in each MLT-L shell bin. Bins with less than 10 microbursts are white. A clear pattern is evident here, with closely spaced microbursts located primarily in the dawn sector and at low L shells, while microbursts further separated in time occur primarily after 12 MLT. The repetition period grows longer

10.1029/2023GL104663

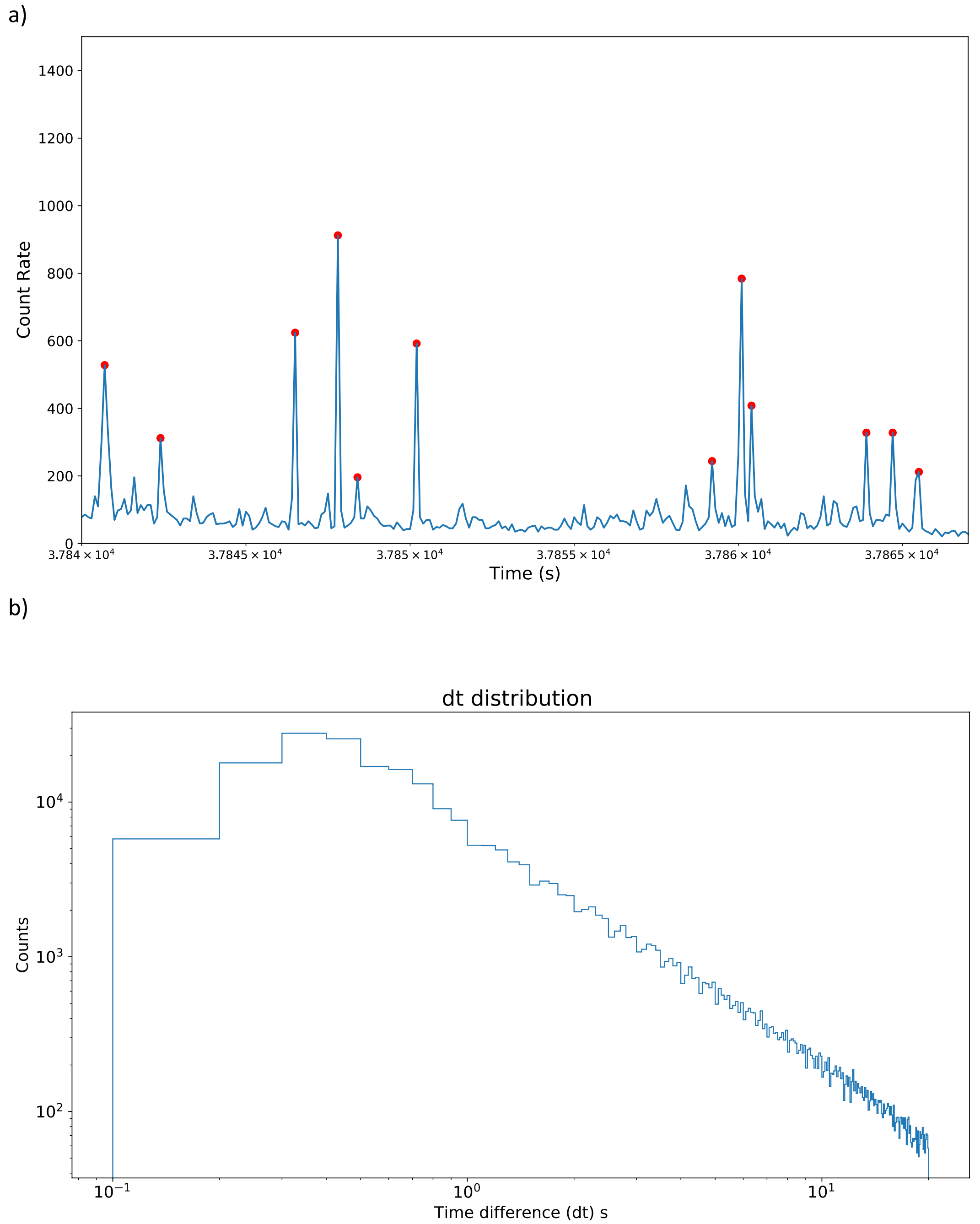

Figure 1. (a) Count rates from Solar, Anomalous, Magnetospheric Particles Explorer Heavy Ion Large Telescope (blue) with microbursts detected by the O'Brien (2003) algorithm (red). The space between the microburst detections represents the repetition period (dt). (b) Distribution of the time difference between neighboring microbursts in seconds, with both axes on a log scale. Most microbursts occur less than one second apart.

as one moves around in MLT from midnight to noon and to larger L shells. Isolated microbursts, with unusually longer dt ~ 10 s, are often observed at L ~ 6 in the afternoon sector.

3.2. AE Dependence

Next, we look at the dependencies of dt on geomagnetic activity, specifically the AE index. Here we sort the microbursts into three categories—those occurring within 1 s of another microburst, those between 1 and 10 s

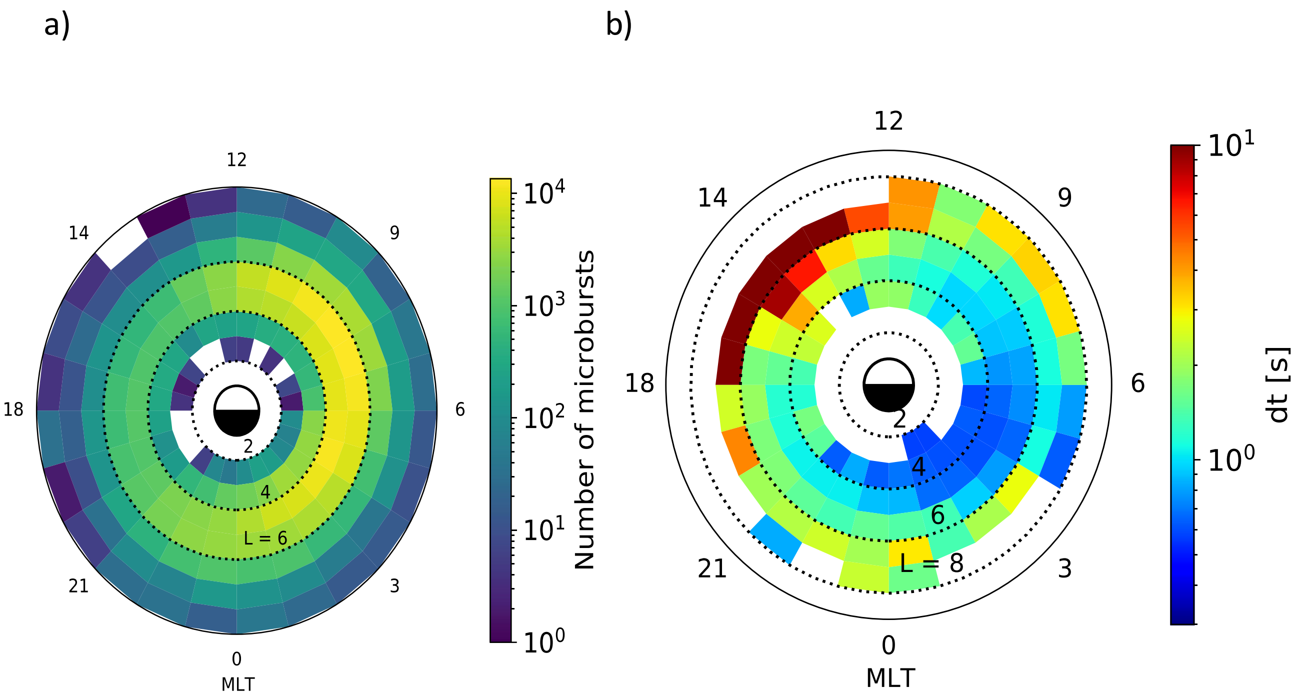

Figure 2. (a) Distribution of microbursts in L shell and magnetic local time (MLT). (b) Distribution of the median dt in each MLT and L shell bin. Bins with less than 10 microbursts are white.

of another microburst, and those >10 s from other microbursts. Figure 3 shows the microburst repetition period probability density function in each of those AE categories. The width of the AE bins is set to be 50 nT.

The results from Figure 3 reveal that microburst repetition period has an AE dependency as well. We see that for the dt category of >10 s (red) the curve peaks at 309 nT in AE, while for the dt category of <1 s (blue) the curve peaks at 559 nT in AE. Thus, during active times, when AE is larger, closely spaced microbursts are

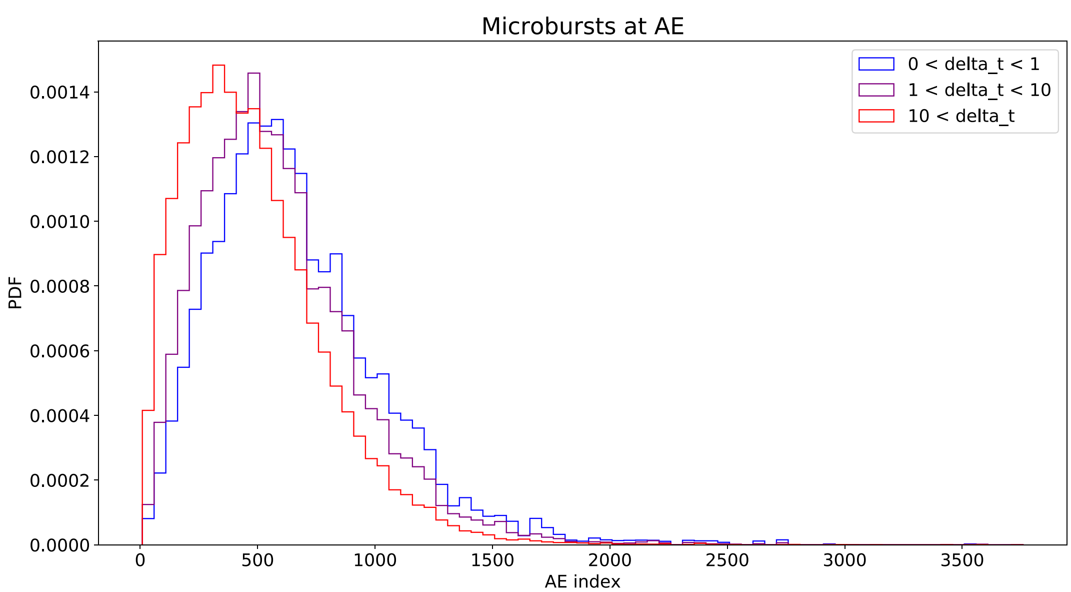

Figure 3. Normalized distribution of the number of microbursts versus Auroral Electrojet (AE) index in three different dt categories. For the dt < 1 s (Blue) the distribution peaks at a value of 559 nT in AE. For 1 < dt < 10 s (purple) the peak is at 459 nT in AE. Finally for dt > 10 s (red) the peak is 309 nT in AE.

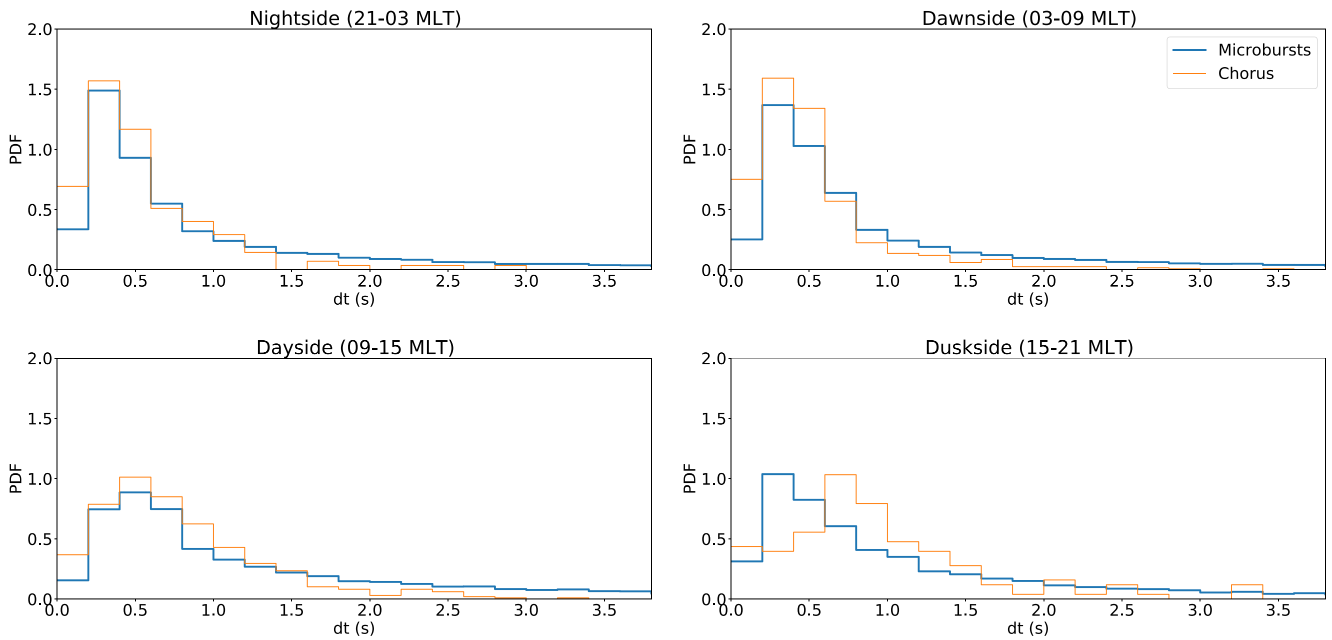

Figure 4. Distributions of the chorus wave (orange) and microbursts (blue) repetition periods in four different magnetic local time categories. Chorus wave distributions are taken from Shue et al. (2015).

more prevalent, while occurrences of more isolated microbursts peak during lower AE values. A similar pattern emerges when microbursts are arranged based on the AL index, with closely saced microbursts peaking during more active times.

4. Discussion

The results above show clear dependencies of microburst repetition period on MLT, L shell, and AE. To better understand potential causes of these trends in the microburst repetition period, we compare to past studies of this similar repetition period property for chorus waves.

Shue et al. (2015) and Gao et al. (2022) have explored the dependence of rising tone chorus element repetition periods on MLT and both studies found a strong dependence similar to that shown here. Chorus wave repetition periods were shortest in the night and dawn sectors, and longer on the day and duskside. Background magnetic field strength and electron temperature were found to be controlling factors for this chorus repetition period (Shue et al., 2015). Gao et al. (2022) observed an inverse correlation between chorus repetition period and the drift velocity of electrons, suggesting faster drifting electrons produce more rapidly repeating chorus wave elements. Thus the electron refilling rate in a given region, from freshly injected particles on the nightside, directly controls chorus element density (or repetition periods).

The power law distribution is the most suitable model for characterizing the repetition period distribution of microbursts, aligning with the findings of Trakhtengerts et al. (2004) regarding chorus elements measured by the Cluster spacecraft. From Figure 1 though, the slope of the full distribution of microbursts was found to be ~(−1.48), which is considerably smaller than that reported by Trakhtengerts et al. (2004). However, Figures 2 and 3 show that this microburst distribution is highly dependent on MLT, L shell, and AE, as are the repetition periods of chorus waves.

Thus for more direct comparison between microburst and chorus repetition period distribution, Figure 4 shows probability distribution function of microburst dt's (blue) overlaid with that of chorus waves as derived from Shue et al. (2015) (orange) for the four different MLT sectors. We find very close agreement between these microburst and chorus wave distributions in the night (21–3 hr), dawn (03–09 hr), and day (09–15 hr) MLT sectors, suggesting chorus wave repetition periods are likely directly controlling those of microburst precipitation. This similarity between chorus wave and microburst properties also likely explains the AE dependences found in Figure 3. The refilling rate of freshly injected electrons on the nightside, which provide the free energy for chorus wave generation, is higher during more active geomagnetic conditions, thus resulting in higher repetition period microbursts as compared to quiet times.

Interestingly, we find that the distributions on the duskside (15–21 hr in MLT) do not show the same agreement, indicating that the dusk side microbursts properties may be controlled by processes other than interaction with chorus wave. Meyer-Reed et al. (2023), looking at the pitch angle anisotropy of microbursts rather than repetition period, also found that duskside microburst properties differed from those in other local time sectors. There have also been a few case studies suggesting EMIC waves, rather than chorus waves, may be a possible source of MeV electron microbursts in the dusk sector (e.g., Douma et al., 2017; Shumko et al., 2022). Further investigation into the drivers of dusk-side MeV electron microburst precipitation is needed to better understand the difference demonstrated in Figure 4 between the precipitation properties and those of chorus waves.

5. Summary

Here we examine 15 years of SAMPEX data to better understand the detailed properties of MeV electron microbursts, particularly their repetition periods, for the first time. We find:

1. Microburst repetition periods are most often <1 s, the distribution follows a decaying power law.
2. Repetition periods show clear dependencies on MLT, L shell, and AE. The periods peaks near noon and $L = 4–6$, and tend to be shorter for higher AE.
3. The distribution of microburst dt's shows very strong agreement with that of chorus wave rising tone elements in the night, dawn, and day-side MLT sectors, while dusk-side distributions do not match well.

These findings illustrate the insight to be gained from exploring the detailed properties of MeV electron microbursts. The repetition period distributions found here highlight the close connection between chorus wave properties and MeV microburst properties on the night, dawn, and day-sides of the magnetosphere, and provide insight into the magnetospheric conditions controlling the trains of microburst precipitation often observed. These findings also reveal the unusual repetition periods of dusk-sector microbursts, suggesting potentially different generation mechanisms or plasma properties mediating the wave-particle interactions in this sector play a role.

Data Availability Statement

The sampex data center at Caltech has provided the data which is accessible to the public and available at SAMPEX/HILT (2013) and (Shumko, M., 2020).

Acknowledgments
This work was supported in part by NASA's H-SR award 80NSSC21K1682, as well as the NASA/Goddard ISFM Space Precipitation Impacts (SPI) team, Grant HISFM21. LC acknowledges the support of NASA Grant 80NSSC21K1320.

References

Baker, D. N., Mason, G. M., Figueroa, O., Colon, G., Watzin, J. G., & Aleman, R. M. (1993). An overview of the solar anomalous, and Magnetospheric Particle Explorer (SAMPEX) mission. *IEEE Transactions on Geoscience and Remote Sensing*, *31*(3), 531–541. https://doi.org/10.1109/36.225519

Blum, L., Li, X., & Denton, M. (2015). Rapid Mev electron precipitation as observed by Sampex/hilt during high-speed stream-driven storms. *Journal of Geophysical Research: Space Physics*, *120*(5), 3783–3794. https://doi.org/10.1002/2014ja020633

Breneman, A. W., Crew, A., Sample, J., Klumpar, D., Johnson, A., Agapitov, O., et al. (2017). Observations directly linking relativistic electron microbursts to Whistler Mode Chorus: Van Allen probes and Firebird II. *Geophysical Research Letters*, *44*(22), 11265. https://doi.org/10.1002/2017gl075001

Chen, L., Zhang, X. J., Artemyev, A., Angelopoulos, V., Tsai, E., Wilkins, C., & Horne, R. B. (2022). Ducted Chorus waves cause sub-relativistic and relativistic electron microbursts. *Geophysical Research Letters*, *49*(5), e2021GL097559. https://doi.org/10.1029/2021gl097559

Crew, A. B., Spence, H. E., Blake, J. B., Klumpar, D. M., Larsen, B. A., O'Brien, T. P., et al. (2016). First multipoint in situ observations of electron microbursts: Initial results from the NSF FIREBIRD II mission. *Journal of Geophysical Research: Space Physics*, *121*(6), 5272–5283. https://doi.org/10.1002/2016ja022485

Douma, E., Rodger, C. J., Blum, L. W., & Clilverd, M. A. (2017). Occurrence characteristics of relativistic electron microbursts from Sampex observations. *Journal of Geophysical Research: Space Physics*, *122*(8), 8096–8107. https://doi.org/10.1002/2017ja024067

Duderstadt, K. A., Huang, C.-L., Spence, H. E., Smith, S., Blake, J. B., Crew, A. B., et al. (2021). Estimating the impacts of radiation belt electrons on atmospheric chemistry using Firebird II and Van Allen probes observations. *Journal of Geophysical Research: Atmospheres*, *126*(7), e2020JD033098. https://doi.org/10.1029/2020jd033098

Elliott, S. S., Breneman, A., Colpitts, C., Bortnik, J., Jaynes, A., Halford, A., et al. (2022). Understanding the properties, wave drivers, and impacts of electron microburst precipitation: Current understanding and critical knowledge gaps. *Frontiers in Astronomy and Space Sciences*, *9*, 1062422. https://doi.org/10.3389/fspas.2022.1062422

Gao, X., Chen, R., Lu, Q., Chen, L., Chen, H., & Wang, X. (2022). Observational evidence for the origin of repetitive chorus emissions. *Geophysical Research Letters*, *49*(12), e2022GL099000. https://doi.org/10.1029/2022gl099000

Horne, R. B., & Thorne, R. M. (2003). Relativistic electron acceleration and precipitation during resonant interactions with Whistler-Mode Chorus. *Geophysical Research Letters*, *30*(10), e2019JA027465. https://doi.org/10.1029/2003gl016973

Klecker, B., Hovestadt, D., Scholer, M., Arbinger, H., Ertl, M., Kastele, H., et al. (1993). Hilt: A heavy ion large area proportional counter telescope for solar and anomalous cosmic rays. *IEEE Transactions on Geoscience and Remote Sensing*, *31*(3), 542–548. https://doi.org/10.1109/36.225520

Lorentzen, K. R., Looper, M. D., & Blake, J. B. (2001). Relativistic electron microbursts during the gem storms. *Geophysical Research Letters*, *28*(13), 2573–2576. https://doi.org/10.1029/2001gl012926

Meyer-Reed, C., Blum, L., & Shumko, M. (2023). Pitch angle isotropy of relativistic electron microbursts as observed by SAMPEX/Hilt: Statistical and storm-time properties. *Journal of Geophysical Research: Space Physics*, *128*(1), e2022JA030926. https://doi.org/10.1029/2022ja030926

Miyoshi, Y., Saito, S., Kurita, S., Asamura, K., Hosokawa, K., Sakanoi, T., et al. (2020). Relativistic electron microbursts as high-energy tail of pulsating Aurora electrons. *Geophysical Research Letters*, *47*(21), e2020GL090360. https://doi.org/10.1029/2020gl090360

Mozer, F. S., Agapitov, O. V., Blake, J. B., & Vasko, I. Y. (2018). Simultaneous observations of lower band chorus emissions at the equator and microburst precipitating electrons in the ionosphere. *Geophysical Research Letters*, *45*(2), 511–516. https://doi.org/10.1002/2017gl076120

Nakamura, R., Isowa, M., Kamide, Y., Baker, D. N., Blake, J. B., & Looper, M. (2000). SAMPEX observations of precipitation bursts in the outer radiation belt. *Journal of Geophysical Research*, *105*(A7), 15875–15885. https://doi.org/10.1029/2000JA900018

O'Brien, T. P. (2003). Energization of relativistic electrons in the presence of ULF Power and MeV microbursts: Evidence for dual ULF and VLF acceleration. *Journal of Geophysical Research*, *108*(A8), 1329. https://doi.org/10.1029/2002ja009784

O'Brien, T. P., Looper, M. D., & Blake, J. B. (2004). Quantification of relativistic electron microburst losses during the GEM storms. *Geophysical Research Letters*, *31*(4), L04802. https://doi.org/10.1029/2003GL018621

Saito, S., Miyoshi, Y., & Seki, K. (2012). Relativistic electron microbursts associated with whistler chorus rising tone elements: GEMSIS-RBW simulations. *Journal of Geophysical Research*, *117*(A10), A10206. https://doi.org/10.1029/2012JA018020

SAMPEX/HILT. (2013). SAMPEX HILT online data repository [Dataset]. Caltech. Retrieved from https://izw1.caltech.edu/sampex/DataCenter/index.html

Seppälä, A., Douma, E., Rodger, C., Verronen, P., Clilverd, M. A., & Bortnik, J. (2018). Relativistic electron microburst events: Modeling the atmospheric impact. *Geophysical Research Letters*, *45*(2), 1141–1147. https://doi.org/10.1002/2017GL075949

Shue, J. H., Hsieh, Y. K., Tam, S. W., Wang, K., Fu, H. S., Bortnik, J., et al. (2015). Local time distributions of repetition periods for rising tone lower band chorus waves in the magnetosphere. *Geophysical Research Letters*, *42*(20), 8294–8301. https://doi.org/10.1002/2015gl066107

Shumko, M. (2020). SAMPEX HILT microburst catalog [Dataset]. GitHub. Retrieved from https://github.com/mshumko/sampex_microburst_widths/data

Shumko, M., Blum, L. W., & Crew, A. B. (2021). Duration of individual relativistic electron microbursts: A probe into their scattering mechanism. *Geophysical Research Letters*, *48*(17), e2021GL093879. https://doi.org/10.1029/2021gl093879

Shumko, M., Gallardo-Lacourt, B., Halford, A. J., Blum, L. W., Liang, J., Miyoshi, Y., et al. (2022). Proton Aurora and relativistic electron microbursts scattered by electromagnetic ion cyclotron waves. *Frontiers in Astronomy and Space Sciences*, *9*, 975123. https://doi.org/10.3389/fspas.2022.975123

Shumko, M., Johnson, A. T., Sample, J. G., Griffith, B. A., Turner, D. L., O'Brien, T. P., et al. (2020). Electron microburst size distribution derived with AeroCube-6. *Journal of Geophysical Research: Space Physics*, *125*(3), e2019JA027651. https://doi.org/10.1029/2019ja027651

Shumko, M., Sample, J., Johnson, A., Blake, B., Crew, A., Spence, H., et al. (2018). Microburst scale size derived from multiple bounces of a microburst simultaneously observed with the Firebird-II CubeSats. *Geophysical Research Letters*, *45*(17), 8811–8818. https://doi.org/10.1029/2018gl078925

Thorne, R. M., O'Brien, T. P., Shprits, Y. Y., Summers, D., & Horne, R. B. (2005). Timescale for MeV electron microburst loss during geomagnetic storms. *Journal of Geophysical Research*, *110*(A9), A09202. https://doi.org/10.1029/2004JA010882

Trakhtengerts, V. Y., Demekhov, A. G., Titova, E. E., Kozelov, B. V., Santolik, O., Gurnett, D., & Parrot, M. (2004). *Interpretation of cluster data on chorus emissions using the backward wave oscillator model*. AIP Publishing. Retrieved from https://pubs.aip.org/aip/pop/article/11/4/1345/104894/Interpretation-of-Cluster-data-on-chorus-emissions